Article ID: 1006-8775(2016) 03-0265-12

STUDY ON THE GENESIS OF ASYMMETRICAL DISTRIBUTION CHARACTERISTICS OF PRECIPITATION ASSOCIATED WITH THE TYPHOON HAITANG (2005) FROM THE VIEW OF ATMOSPHERIC FACTOR

YUE Cai-jun (岳彩军)[1], CAO Yu (曹 钰)[2], GU Wen (顾 问)[1], TAN Jian-guo (谈建国)[1], LI Xiao-fan (李小凡)[3]
(1. Shanghai Institute of Meteorological Science(Shanghai Satellite Remote-Sensing and Application Centre), Shanghai 200030 China; 2. Yangtze River Delta Center for Environmental Meteorology Prediction and Warning (Shanghai Center for Environmental Meteorology), Shanghai 200030 China;
Department of Earth Sciences, Zhejiang University, Hangzhou 310027 China)

Abstract: The distribution of precipitation field from the typhoon Haitang (2005) during its landing on Fujian province shows obvious asymmetric feature. Based on the NCEP/NCAR FNL (Final Analysis) data, this study reveals the contributions of atmospheric factor to the asymmetrical distribution characteristics of precipitation associated with the typhoon, through the analysis of water vapor condition, vertical ascending motion condition, the calculation of the dry Q vector and its decomposition, and adiabatic heating in the air column of 1000hPa-600hPa (lower atmosphere) and 500hPa-100hPa (upper atmosphere). The results are as follows: (1) In the lower atmosphere, the humidity on both sides of typhoon path can be equivalent, while it is more wet on the right side than left in the upper atmosphere, which obviously presents asymmetric distribution characteristics. (2) Both range and intensity of the vertical motion on the right side are wider and stronger than counterparts on the left side no matter in the lower or upper atmosphere. (3) In the upper atmosphere, forcing role of atmosphere in vertical upward motion on the right side of typhoon path is the same as that on the left, while it is significantly different in the lower atmosphere, which is significantly broader in scope and stronger in the intensity, along with obvious asymmetric distribution characteristics. In addition, the further analysis of the Q vector decomposition indicates that the forcing effect of mesoscale weather systems on vertical upward motion is stronger than that of large scale weather systems in the lower atmosphere. (4) The adiabatic heating always exists on both lower and upper atmosphere, and the range and intensity of the adiabatic heating forcing showed asymmetric distribution on both lower and upper atmosphere. (5) In a summary, the upper atmosphere humidity conditions, the forcing role of lower atmosphere in vertical upward motion, especially, to mesoscale weather system, and adiabatic heating in the lower atmosphere, all show similar asymmetric distribution characteristics to that of precipitation field from the typhoon Haitang (2005), that is to say, the atmospheric factors as mentioned above are all contributed to genesis of the asymmetric distribution characteristics of precipitation.

Key words: asymmetric distribution characteristics; water vapor condition; vertical upward motion; Q vector; adiabatic heating
CLC number: P444 **Document code:** A
doi: 10.16555/j.1006-8775.2016.03.001

1 INTRODUCTION

Landfall tropical cyclone (TC) usually leads to the obvious precipitation. According to the land records, distribution of precipitation associated with TC is often asymmetric, with no obvious circular features, especially the torrential rainstorm or extraordinary rainstorm distribution is very uneven and changeable. Scholars at home and abroad carried out a wide range of related research of TC's precipitation distribution characteristics and its cause, along with observation, diagnostic analysis and numerical simulation. Based on a large number of observations, Chen et al. and Cheng et al. pointed out that the range and intensity of heavy rain from majority TC landed in the right semicircle is significantly greater than counterparts in the left half[1-3]. Based on the composite analysis of landing TC's precipitation observations, some researchers (Cline[4]; Koteswaram and Gaspar[5]; Miller[6]; Frank[7]) suggested that landfall TC's rainfall distribution is obviously asymmetric, and the maximum precipitation mainly located in the TC's right-front side. However, there are also the opposite conclusions, Parrish et al. and Elsberry found that the maximum precipitation is located in the left-front side of landing TC[8, 9]. What is more, Burpee and Black found that the change of asymmetric

Received 2014-10-31; **Revised** 2016-06-12; **Accepted** 2016-07-15
Foundation item: National Natural Science Foundation of China (40875025, 41175050, 41275021, 41475039, 41475041, 41575048); Public Sector (Meteorology) Research of China (GYHY201306012, GYHY201506007)
Biography: YUE Cai-jun, Ph.D., Researcher, primarily undertaking research on mesoscale dynamics and air-sea interaction.
Corresponding author: YUE Cai-jun, e-mail: yuecaijun 2000@ 163.com

characteristics of landfall TC's precipitation existed in some way, and the location of the maximum precipitation moved from TC's left side to the right side [10]. The above analysis showed that the complexity of the TC's precipitation distribution is obvious. This also came from the complexity of the reasons that the heavy rain of landing typhoon took place. It involved the typhoon circulation structure, strength, track, moving speed, environment field, underlying surface and so on. We can see that analysis of the formation reason with the asymmetric distribution characteristics of precipitation associated with typhoon was feasible on the basis of atmospheric factor. Tao et al. analyzed the relationship between the asymmetry of the flow field and thermal field structure and the formation of torrential rain by the routine observation after the typhoon Polly (9216) landed [11]. Ding et al. studied the effects of asymmetric structure of typhoon Doug (9414) on precipitation by using large-scale weather system configuration, satellite cloud image and the results of numerical simulation [12]. Recently, using quasi-geostrophic Q vector, Atallah et al. analyzed the dynamics reason that distribution of precipitation from tropical cyclones was asymmetric after their landfall in the eastern US [13]. In addition, in order to reveal the reasons for the formation of asymmetric distribution of precipitation caused by landfall TC, there were also many meteorologists (Tuleya and Kurihara [14]; Bender et al. [15]; Wu et al.[16]; Chen and Yau [17]; Lv et al.[18]; Yuan et al.[19]; Ding et al.[20]; Wang et al.[21]; Xu et al.[22]) to carry out related research through the (ideal) numerical simulation method. Obviously, the above researches have made some progress.

As we all know, the distribution of precipitation from typhoon Haitang (2005) was asymmetric markedly. Yue et al. found that Haitang (2005) circulation structures on land had a characteristic of the north-south asymmetric distribution by using hourly infrared IR1 images [23]. They also found that contributions from dynamic factor were much more obvious than the counterparts from thermodynamic factor. Later, Yue made a further quantitative research based on the results of numerical simulation and thought that asymmetric distribution caused by atmospheric factor forcing could lead to asymmetric characteristics of vertical ascending motion to format, then it leaded to the formation of the asymmetrical characteristic of precipitation, on the other hand, it could bring out terrain factor to play an important role, the final result made the asymmetric characteristics of precipitation in the whole process of typhoon become further obvious [24]. However, the forcing role of the atmospheric factor were both based on moisture condition and vertical ascending motion at 700 hPa[23, 24]. For the atmospheric factor throughout the whole column, what about its effect? In order to further reveal that the atmospheric factor's role in the formation of asymmetric characteristics during the precipitation process of typhoon Haitang (2005), this study will started from water vapor and upward motion in upper (500 hPa-100 hPa) and lower (1000 hPa-600 hPa) atmosphere, along with calculating ageostrophic dry Q vector, its decomposition and diabatic heating, then dynamic and thermodynamic forcing within the upper and lower atmosphere and the forcing effects of different scale weather systems will be analyzed concretely and carefully, which is contributed to help us understand the effect of the atmospheric factor on the formation of asymmetric characteristics during the precipitation process of typhoon Haitang (2005).

2 DISTRIBUTION FEATURE OF PRECIPITATION FROM TYPHOON HAITANG (2005) AND BRIEF INTRODUCTION TO DATA

2.1 *Distribution feature of precipitation*

Typhoon Haitang (2005) landed in the island of Taiwan, and then it landed again at Huangqi town, Lianjiang city, Fujian province at 1710 Beijing Standard Time (BST) 19 July 2005. As in Fig.1a, typhoon Haitang (2005) moved southwestward during 0800BST 19-0800BST 20 July 2005, with obvious precipitation (Fig.1b). It is noteworthy that torrential rainfall occurred over the northeast coast of Fujian province, and the coast and north of Zhejiang province, which were at the right side of typhoon path, and the precipitation on the left side of typhoon path was obviously lighter. Therefore, typhoon path taken as reference standard of comparative analysis, the range and intensity of 24-h accumulated precipitation show the obvious asymmetric distribution feature. As in Fig.2, the range and intensity of 6-h accumulated precipitation presents similar asymmetric distribution feature to that in Fig.1b, which further shows that the asymmetric distribution feature of precipitation is continuous.

Here it is needed to say specially that the typhoon path (Fig.1a) is mainly takes as reference standard to analyze asymmetric distribution feature related to physical quantities, and the difference of range and intensity of physical quantities between in Fujian province and Zhejiang province on the right side of typhoon path and in Fujian province on the left side of typhoon path is analyzed qualitatively.

2.2 *Data*

The analysis is based on the NCEP/NCAR Final Analysis data with time interval of 6h, horizontal resolution of 1°×1° and vertical resolution of 21 layers (1000hPa, 975hPa, 950hPa, 925hPa, 900hPa, 850hPa, 800hPa, 750hPa, 700hPa, 650hPa, 600hPa, 550hPa, 500hPa, 450hPa, 400hPa, 350hPa, 300hPa, 250hPa, 200hPa, 150hPa, 100hPa). For convenient analysis, air column of 1000-600 hPa and 500-100 hPa is used to represent lower and upper atmosphere, respectively, and the period from 0800 BST 19 July to 0800 BST 20 July 2005 is taken as the main analyzed period. Meanwhile, the analysis range mainly targets mainland of China,

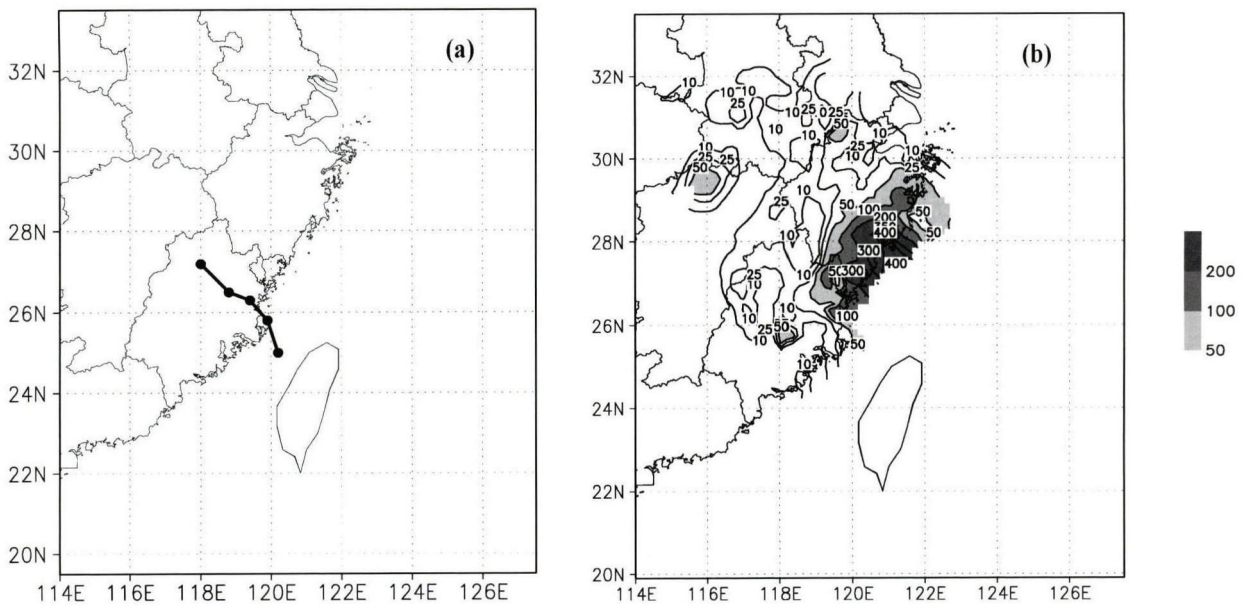

Figure 1. (a) Positions and (b) observed 24 hours accumulated precipitation amount (mm) for typhoon Haitang during 0800 BST 19 Jul to 0800 LST 20 Jul 2005.

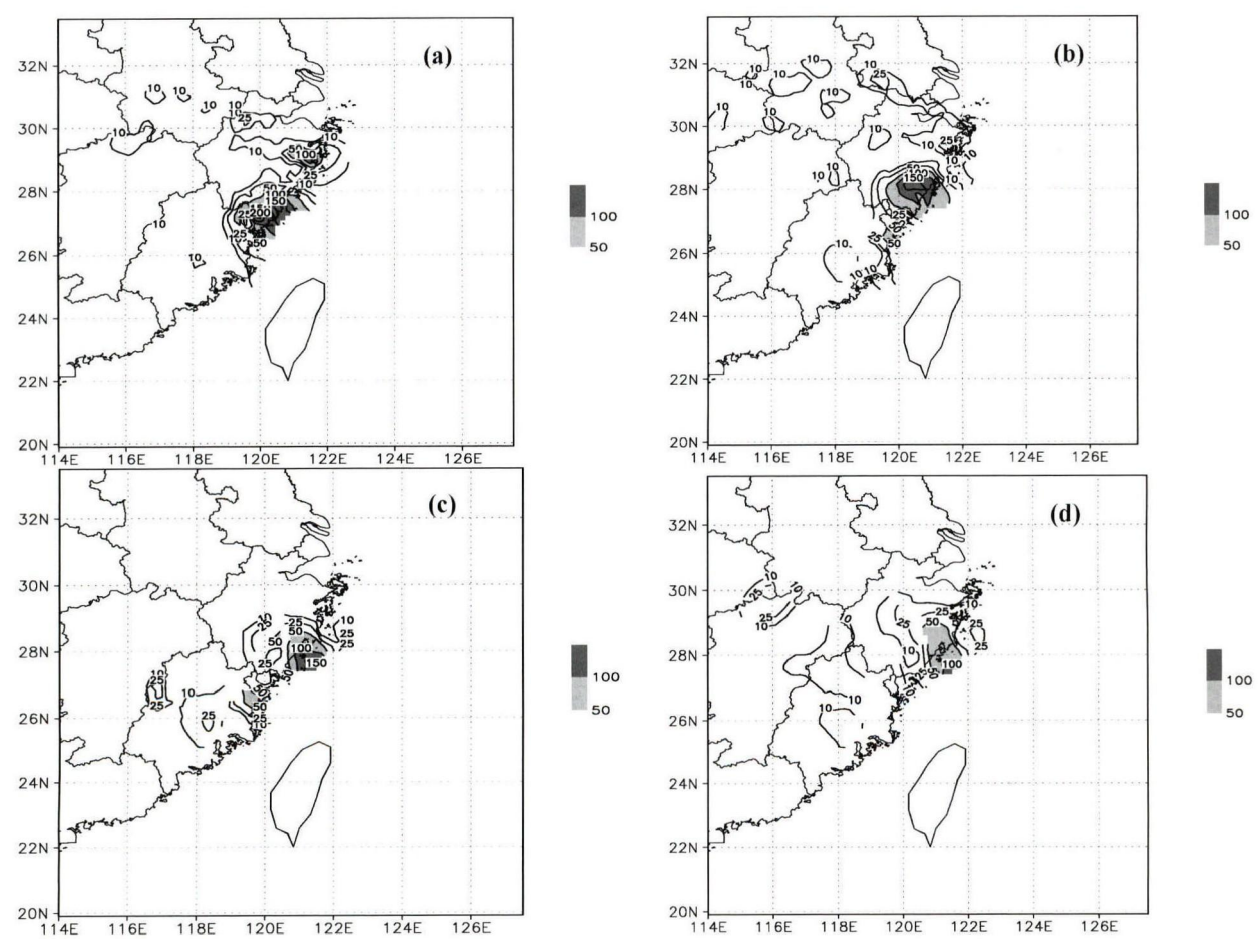

Figure 2. Each observed 6 hours accumulated precipitation amount (mm) for typhoon Haitang at 1400 BST 19 Jul (a), 2000 BST 19 Jul (b), 0200 BST 20 Jul (c) and 0800 BST 20 Jul (d) 2005 (shaded areas represent intensity of precipitation over 50mm/6h).

excluding Taiwan province and oversea.

3 ANALYSIS OF WATER VAPOR CONDITION

As we all know, water vapor condition is one of the important conditions for precipitation occurrence. Firstly, the horizontal distribution feature of average relative humidity RH≥70% in lower atmosphere (1 000–600hPa) from 0800 BST 19 July to 0800 BST 20 July 2005 is analyzed. For convenient analysis, average relative humidity with intensity of RH≥70%, 80% and 90% are marked as RH_{70}, RH_{80} and RH_{90}, respectively. As in Fig.3, RH_{70} and RH_{80} on both sides of typhoon path do not present asymmetric distribution, and the asymmetric distribution of RH_{90} is not obvious. So we can see that none of RH_{70}, RH_{80} and RH_{90} present asymmetric distribution feature as in Fig.1b and Fig.2, which is similar to Yue's[24] conclusion of "Neither RH_{80} nor RH_{90} presents asymmetric distribution at 700 hPa".

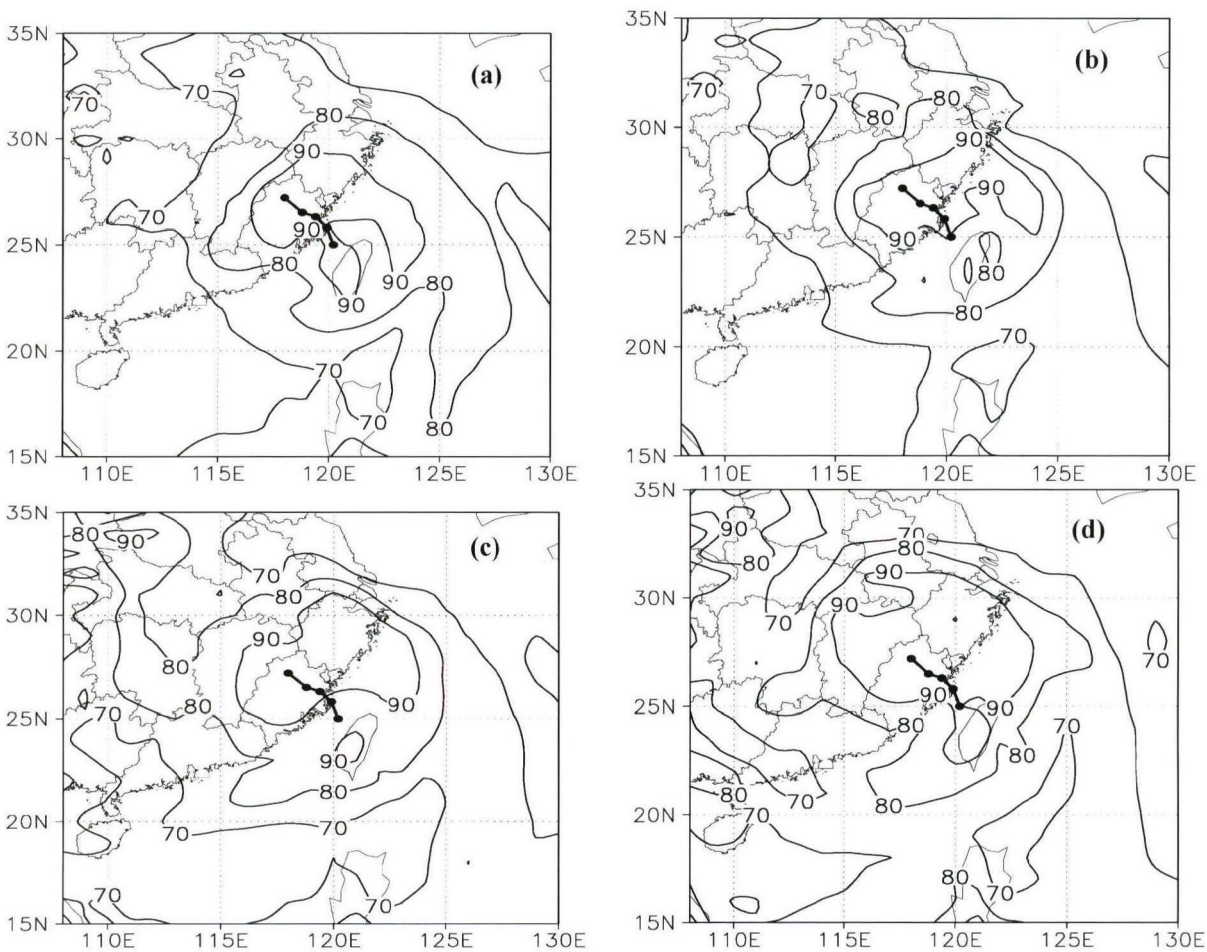

Figure 3. Averaged relative humidity in 1000 to 600hPa air column at 1400 BST 19 Jul (a), 2000 BST 19 Jul (b), 0200 BST 20 Jul (c) and 0800 BST 20 Jul (d) 2005 (positions represent track of typhoon Haitang).

By further analyzing the horizontal distribution feature (Fig.4) of average relative humidity with intensity of RH ≥70% in upper atmosphere (500-100 hPa), it can be seen that RH_{70} on both sides of typhoon path presents asymmetric distribution basically, and RH_{80} and RH_{90} presents asymmetric distribution feature obviously, with much larger coverage area on the right, which has a good uniformity to asymmetric distribution feature of precipitation in Fig.1b and Fig.2.

The above analysis shows that the humidity condition of lower atmosphere on both sides of typhoon path is almost equivalent, without asymmetric distribution, while in upper atmosphere, the right side of typhoon path is obviously much wetter than the left side, with obvious asymmetric distribution. It may mean that lower atmosphere of typhoon often has good humidity condition, while the distribution feature of the water vapor condition in upper atmosphere may have a good indication to the fallout region and intensity of precipitation.

4 ANALYSIS OF VERTICAL ASCENDING MOTION CONDITION

Vertical ascending motion is another important condition for precipitation occurrence. For convenient analysis, regions of average vertical upward motion with intensity of $|\omega| \geq 0$, $|\omega| \geq 0.1\times10^{-2}$ hPa/s, $|\omega| \geq 0.3\times10^{-2}$ hPa/s and $|\omega| \geq 0.6\times10^{-2}$ hPa/s are marked as W_0, $W_{0.1}$, $W_{0.3}$ and $W_{0.6}$, respectively. By analyzing Fig.5 and Fig.6, it can be known that the range and intensity of vertical

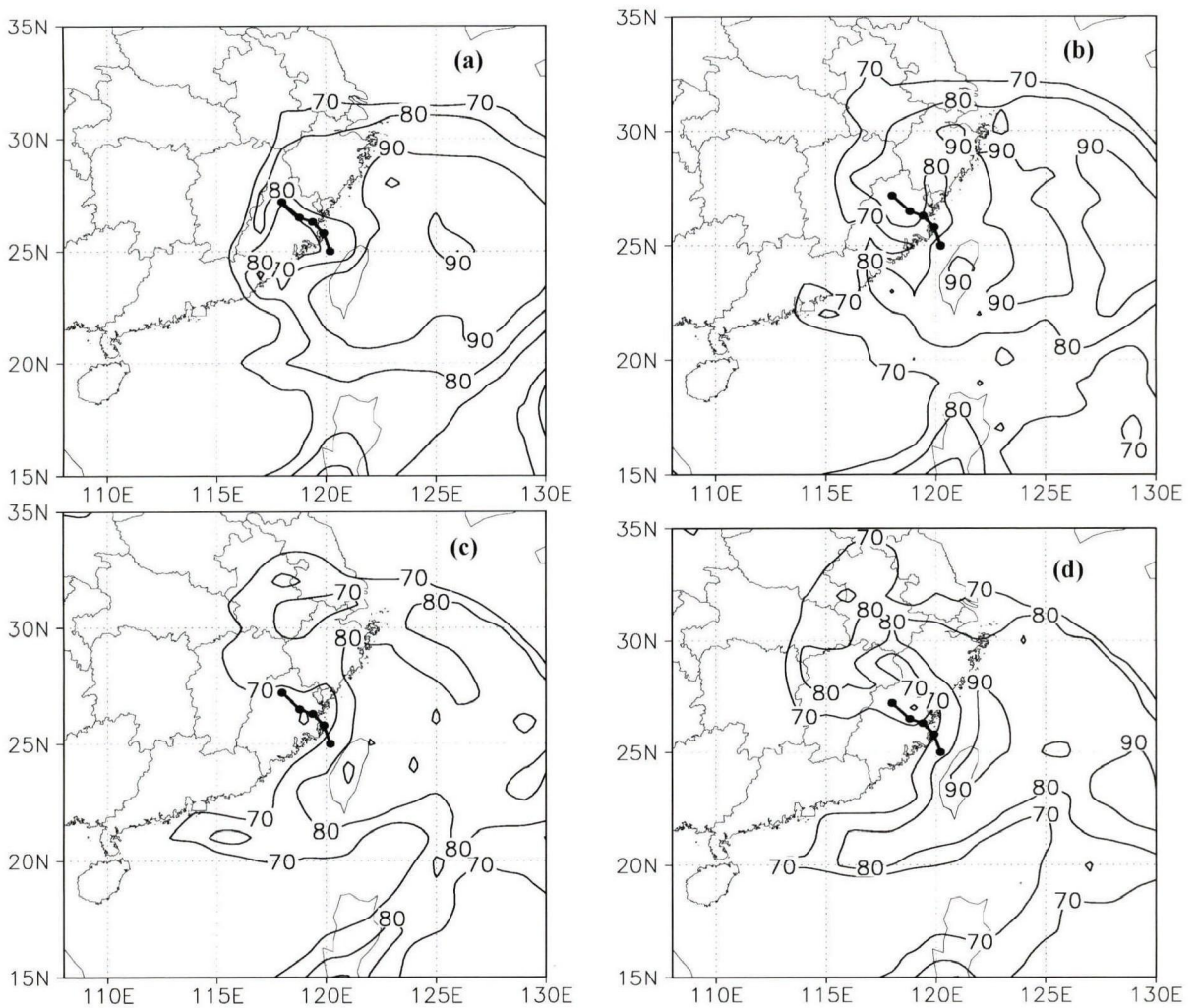

Figure 4. Same as Fig.3, except for 500 to 100hPa air column.

upward motion on both sides of typhoon path present obvious asymmetric distribution feature, with right side larger than that of left side, which has a good coherence to the asymmetric distribution feature of precipitation in Fig.1b and Fig.2. Comparatively, the range and intensity of the vertical upward motion on the right side of typhoon path is wider and stronger than counterparts on the left side, respectively.

5 ANALYSIS OF AGEOSTROPHIC DRY *Q* VECTOR

The vertical upward motion information used in section 4 is from FNL, which is the result from comprehensive analysis, including the information of forcing factors such as terrain, atmosphere and so on. How to reveal the vertical ascending motion forced by the atmospheric factor? As we all know, vertical motion cannot be obtained from the observing method till now, it mainly depends on analysis based on other physical quantities. Q vector includes dynamic and thermodynamic information of atmosphere. Theoretical analysis shows that there is a good correspondence between Q vector divergence and vertical motion under some conditions. Meanwhile, compared with the diagnostic method of solving Omega equation which involves complicated processing as iterative calculation, Q vector analysis method is simple and practical, which is considered as an advanced tool for analyzing vertical motion. The following section will reveal the vertical upward motion distribution feature forced by the atmosphere on the basis of analyzing ageostrophic dry Q vector divergence. As for the forcing effect of diabatic heating on vertical upward motion field will be analyzed in the next section.

5.1 *"Total" Q vector analysis*

Zhang obtained ageostrophic dry Q vector (Q^D) from original equation of quasi-static, adiabatic, non-frictional, f-plane and p-coordinate system, which can be expressed as[25]:

$$Q_x^D = \frac{1}{2}\left[f\left(\frac{\partial v}{\partial p}\frac{\partial u}{\partial x} - \frac{\partial u}{\partial p}\frac{\partial v}{\partial x}\right) - h\frac{\partial \boldsymbol{V}}{\partial x}\cdot\nabla\theta\right] \quad (1)$$

$$Q_y^D = \frac{1}{2}\left[f\left(\frac{\partial v}{\partial p}\frac{\partial u}{\partial y} - \frac{\partial u}{\partial p}\frac{\partial v}{\partial y}\right) - h\frac{\partial \boldsymbol{V}}{\partial y}\cdot\nabla\theta\right] \quad (2)$$

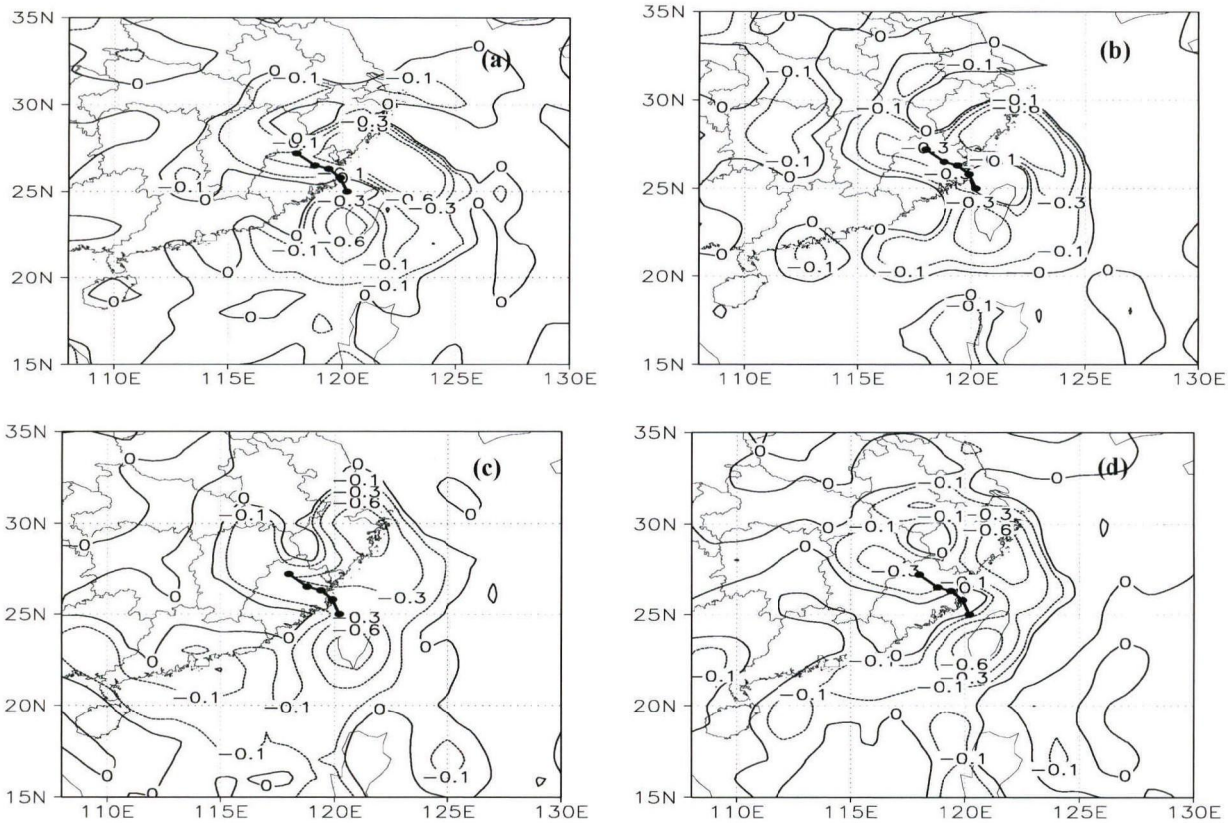

Figure 5. Same as Fig.3, except for vertical velocity (unit: 10^{-2} hPa/s).

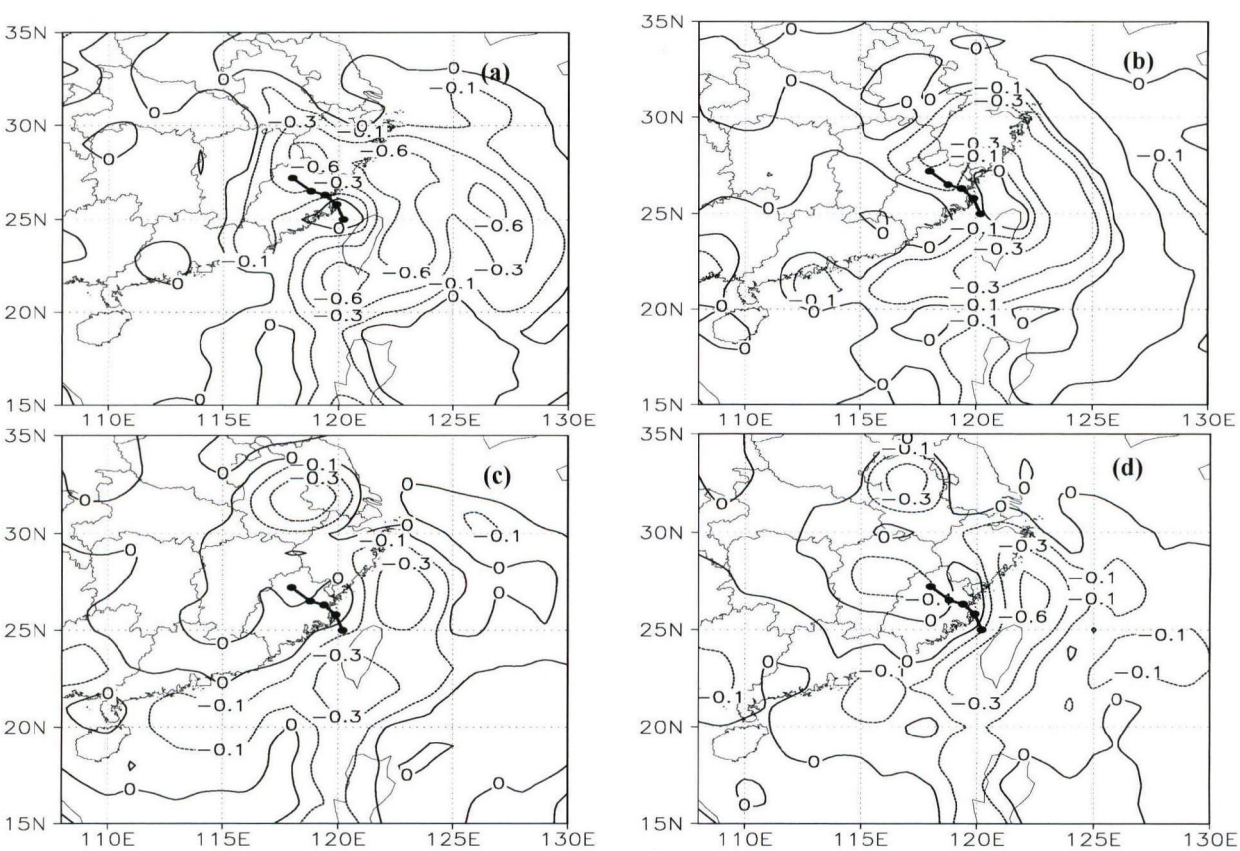

Figure 6. Same as Fig.5, except for vertical velocity at upper level.

where, $h=\frac{R}{p}(\frac{p}{1000})^{R_d/C_p}$, $\theta=T(\frac{1000}{p})^{R_d/C_p}$, $\mathbf{V}=u\boldsymbol{i}+v\boldsymbol{j}$ and others are common physical pa rameters of meteorology.

With Q^D vector divergence as forced item, ageostrophic Omega equation is:

$$\nabla^2(\sigma\omega)+f^2\frac{\partial^2\omega}{\partial p^2}=-2\nabla\cdot\boldsymbol{Q}^D \quad (3)$$

If the ω field has wavelike feature, it can be obtained from Eq.(3):

$$\nabla\cdot\boldsymbol{Q}^D\propto\omega \quad (4)$$

Eq.(4) can be used to evaluate vertical motion. If $\nabla\cdot Q^D<0$, then $\omega<0$, showing ascending motion; if $\nabla\cdot Q^D>0$, then $\omega>0$, showing descending motion.

The following is to analyze horizontal distribution characteristics of the Q^D vector divergence field intensity of $|2\nabla\cdot Q^D|\geqslant 0$ in lower atmosphere. For convenient analysis, regions of Q vector divergence with convergence intensity of $|2\nabla\cdot Q^D|\geqslant 0$, $|2\nabla\cdot Q^D|\geqslant 0.1\times10^{-15}$ hPa/s^3, $|2\nabla\cdot Q^D|\geqslant 0.5\times10^{-15}$ hPa/s^3 and $|2\nabla\cdot Q^D|\geqslant 1.0\times10^{-15}$ hPa/s^3 are marked as Q_0, $Q_{0.1}$, $Q_{0.5}$ and $Q_{1.0}$, respectively. By analyzing Fig.7, it can be known that the range and intensity of Q^D vector divergence con vergence present obvious asymmetric distribution feature, with right side much larger and stronger than counterparts of left side. It shows that the forcing effect of ageostrophic dry Q vector on vertical ascending motion on the right side of typhoon path is much stronger than counterparts on the left side, which has a good coherence to the asymmetric distribution characteristic of precipitation in Fig.1b and Fig.2. By further analyzing the horizontal distribution of average $|2\nabla\cdot Q^D|\geqslant 0$ in upper atmosphere (Figure omitted), it is discovered that the asymmetric feature of both range and intensity of Q^D vector divergence convergence field are not obvious, which shows that the forcing effect of ageostrophic dry Q vector on vertical motion in upper atmosphere on both sides of typhoon path is almost the same, without asymmetric distribution feature. So the forcing effect of ageostrophic dry Q vector on vertical motion in lower atmosphere on the right side of typhoon path is much wider and stronger than counterparts on the left side, with obvious asymmetric distribution.

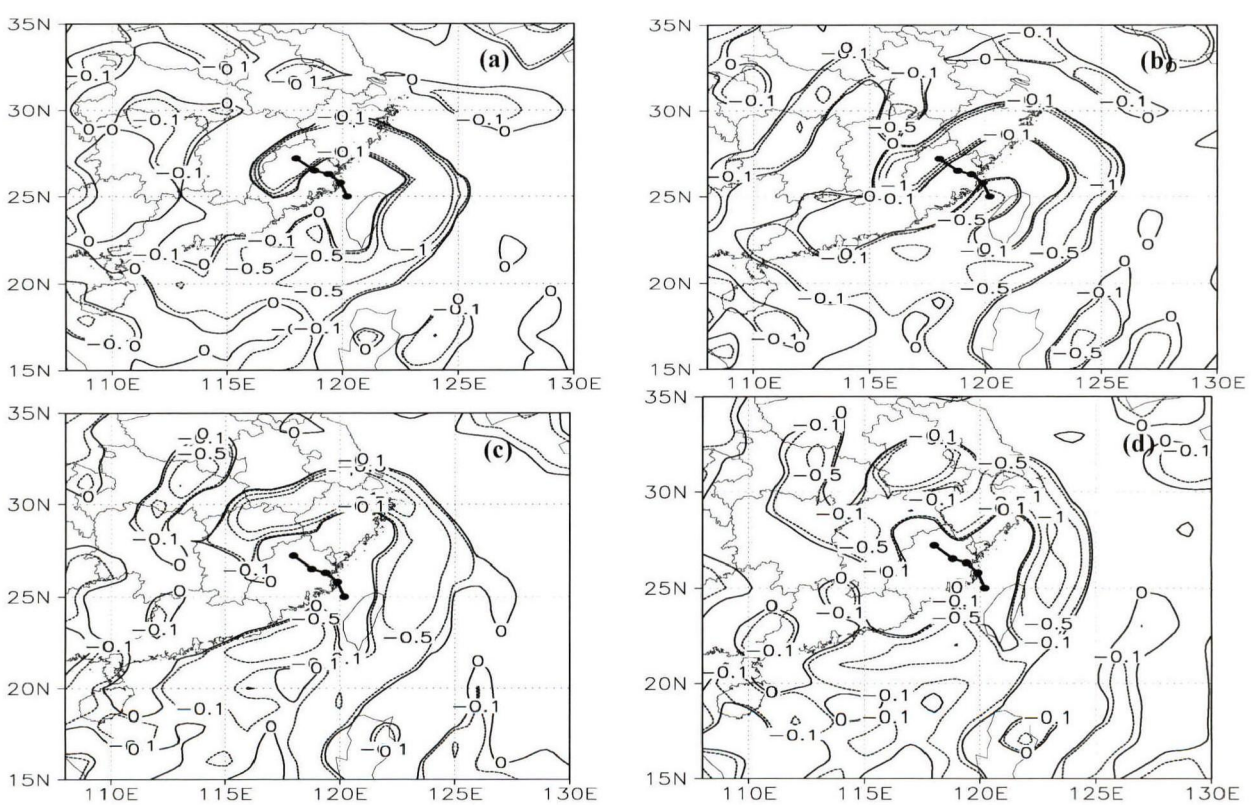

Figure 7. Same as Fig.3, except for convergence field of Q^D vector divergence (unit: 10^{-15}hPa/s).

5.2 *Analysis of Q vector partitioning*

According to the traditional Q vector partitioning method, the ageostrophic dry Q vector was often decomposed into two parts: Q_s was the component along the direction of potential temperature and Q_n was the component along the direction of potential temperature gradient.Q_s represents the thermal wind direction with quasi- geostrophic characteristics, denoting large-scale information; Q_n is the geostrophic departure, denoting the mesoscale weathers (Keyser et

al.[26, 27]; Kurz [28, 29]; Barnes and Colman [30, 31]; Schar and Wernl [32]; Martin [33, 34]; Yue et al.[35-37]; Pyle et al.[38]; Posselt and Martin [39]; Wang et al.[40]; Yang et al.[41]; Thomas and Martin[42]; Liang et al.[43]; Yue[44]).

Q_n^D and Q_s^D have similar diagnostic feature to Q^D, and can be expressed as follows in the p-coordinate system:

$$\boldsymbol{Q}_n^D = [\frac{(\frac{\partial\theta}{\partial x}Q_x^D + \frac{\partial\theta}{\partial y}Q_y^D)\frac{\partial\theta}{\partial x}}{(\frac{\partial\theta}{\partial x})^2 + (\frac{\partial\theta}{\partial y})^2}]\boldsymbol{i} + [\frac{(\frac{\partial\theta}{\partial x}Q_x^D + \frac{\partial\theta}{\partial y}Q_y^D)\frac{\partial\theta}{\partial y}}{(\frac{\partial\theta}{\partial x})^2 + (\frac{\partial\theta}{\partial y})^2}]\boldsymbol{j} \quad (5)$$

$$\boldsymbol{Q}_s^D = [\frac{(\frac{\partial\theta}{\partial y}Q_x^D - \frac{\partial\theta}{\partial x}Q_y^D)\frac{\partial\theta}{\partial y}}{(\frac{\partial\theta}{\partial x})^2 + (\frac{\partial\theta}{\partial y})^2}]\boldsymbol{i} + [\frac{(-\frac{\partial\theta}{\partial y}Q_x^D + \frac{\partial\theta}{\partial x}Q_y^D)\frac{\partial\theta}{\partial x}}{(\frac{\partial\theta}{\partial x})^2 + (\frac{\partial\theta}{\partial y})^2}]\boldsymbol{j} \quad (6)$$

The $2\nabla\cdot Q_n^D$ and $2\nabla\cdot Q_s^D$ will be calculated and analyzed to reveal the forcing effect of different weather scale system in the following.

Based on the diagnostic results from section 5.1, this section will only analyze ageostrophic dry Q vector in the lower atmosphere, with combining "total" Q^D vector divergence convergence field in lower atmosphere in Fig.7. Compared Fig.8 with Fig.7, it can be discovered that the horizontal distribution feature of Q_n^D vector divergence convergence field is similar to that of Q^D vector divergence convergence field on the whole, especially for Q^D vector divergence convergence field with spiral distribu tion feature in Zhejiang province, the distribution characteristic of Q_n^D vector divergence convergence area is extremely similar to that of Q^D vector divergence convergence area, with almost the same strength. Overall, there's difference between horizontal distribution feature of Q_s^D vector divergence convergence field and that of Q^D vector divergence convergence field, especially for the Q^D vector divergence convergence field with spiral distribution in Zhejiang province, which has not been reflected basically in Q_s^D vector divergence convergence field, and the convergence intensity of Q_s^D vector divergence is much weaker than that of Q^D vector divergence. Compared with Q_s^D vector divergence convergence field, Q_n^D vector divergence convergence field is much closer to Q^D vector divergence convergence field in both horizontal distribution feature and convergence intensity, which means that Q_n^D vector is the main component of Q^D vector, and Q_s^D is the secondary factor. Especially for spiral distribution feature of the Q^D vector divergence convergence field in Zhejiang province, which is seen as the main factor causing asymmetric distribution feature of precipitation, the reflecting ability of Q_n^D to it is much better than that of Q_s^D in both horizontal distribution feature and intensity. Meanwhile, combining with the analysis result from section 5.1, it can be considered that forcing effect of mesoscale weather system in low atmosphere is much stronger than that of large-scale weather system, which contributes more to the forming of asymmetric distribution characteristic of precipitation in Fig.1b and Fig.2.

6 ANALYSIS OF DIABATIC HEATING EFFECT

Many studies show that diabatic heating is related closely to precipitation occurrence. Therefore, it is necessary to analyze cause of asymmetric distribution of precipitation from the aspect of diabatic heating. According to the job of Yue et al., the relation between diabatic heating and vertical motion can be expressed as follows[37]:

$$\frac{R_d}{C_p\cdot p}\nabla^2(H) \propto \omega_H \quad (7)$$

where, H is diabatic heating rate, ω_H is the vertical motion forced by diabatic heating in p-coordinate system. Eq.(7) has similar diagnostic feature to Eq.(4). As for H, it includes all heating information such as condensation heating (large-scale condensation heating and convective condensation heating), radiation heating and sensible heating, the equation can be expressed as:

$$H = \frac{d\theta}{dt} = \frac{\partial\theta}{\partial t} + u\frac{\partial\theta}{\partial x} + v\frac{\partial\theta}{\partial y} + \omega\frac{\partial\theta}{\partial p} \quad (8)$$

where, u and v are horizontal wind field, ω is vertical speed, θ is potential temperature, and others are common physical parameters in meteorology. It needs to be specified that ω in Eq.(8) is from FNL. The Laplace of diabatic heating in upper and lower atmosphere will be calculated in order to reveal the forcing effect of diabatic heating on vertical motion. For convenient description, the Laplace of diabatic heating $\frac{R_d}{C_p\cdot p}\nabla^2(H)$

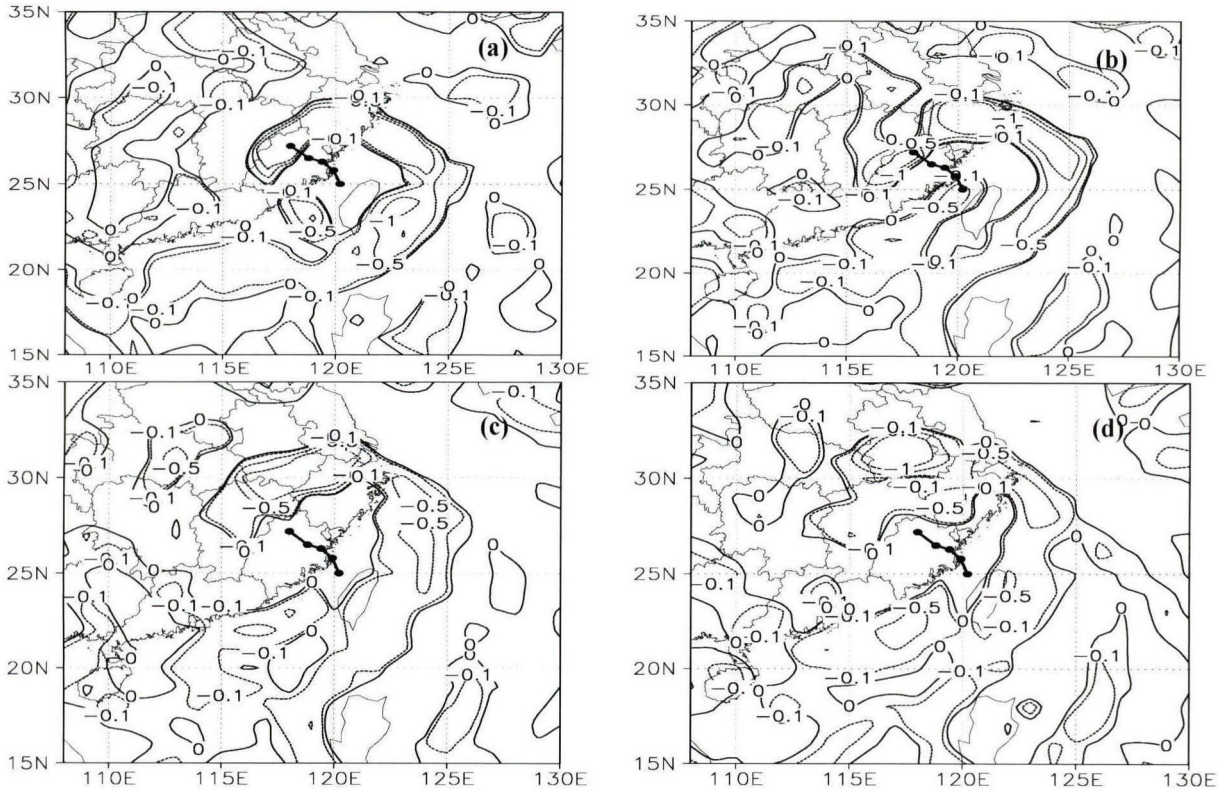

Figure 8. Same as Fig.3, except for convergence field of Q_n^D vector divergence (unit: 10^{-15}hPa/s).

is marked as HD.

Firstly, the forcing effect of diabatic heating in lower atmosphere on vertical ascending motion will be analyzed, i.e., the evolution feature of average $|\frac{R_d}{C_p \cdot p}\nabla^2(H)| \geqslant 0$ regiona in air column will be analyzed. What's more, $|\frac{R_d}{C_p \cdot p}\nabla^2(H)| \geqslant 0$, $|\frac{R_d}{C_p \cdot p}\nabla^2(H)| \geqslant 1.0\times10^{-15}$ hPa/s^3, $|\frac{R_d}{C_p \cdot p}\nabla^2(H)| \geqslant 5.0\times10^{-15}$ hPa/s^3 and $|\frac{R_d}{C_p \cdot p}\nabla^2(H)| \geqslant 10.0\times10^{-15}$ hPa/s^3 are marked as HD_0, $HD_{1.0}$, $HD_{5.0}$ and $HD_{10.0}$, respectively.

From Fig.9, it can be known that the range and intensity of HD convergence on both sides of typhoon's track present obvious asymmetric distribution feature, and the forcing effect of diabatic heating on the right side of typhoon path is wider and stronger than counterparts on the left side, which is consistent with the asymmetric distribution feature of precipitation in Fig.1b and Fig.2. By further analyzing forcing effect of diabatic heating on vertical ascending motion in upper atmosphere (Figure omitted), it can be discovered that HD convergence field in upper atmosphere presents certain asymmetric distribution as well. Above analysis shows that there's diabatic heating effect within upper and lower atmosphere in Fujian province and Zhejiang province on both sides of typhoon path, that is to say, the range and intensity of diabatic heating effect in upper and lower atmosphere present certain asymmetric feature referring to typhoon's track.

7 CONCLUDING REMARKS

For the asymmetric distribution feature of precipitation from typhoon Haitang (2005), based on FNL data, by analyzing water vapor and vertical ascending motion in upper and lower atmosphere, calculating ageostrophic dry Q vector with its partitioning and diabatic heating effect, and taking typhoon path as reference standard, the contributions of atmosphere factor are analyzed. The results are as follows:

(1) The humidity condition in lower atmosphere on both sides of typhoon path is almost equivalent, without asymmetric distribution, however, there is much more vapor in upper atmosphere on the right side of typhoon's track, with obvious asymmetric distribution feature.

(2) The range and intensity of vertical ascending motion in upper and lower atmosphere on the right side of typhoon path is much wider and stronger than counterparts on the left side, with obvious asymmetric distribution feature. By analyzing ageostrophic dry Q vector, it can be discovered that forcing effects of ageostrophic dry Q vector on vertical motion in upper atmosphere on both sides of typhoon path are almost equivalent, and the range and strength of forcing effect of ageostrophic dry Q vector on vertical motion in

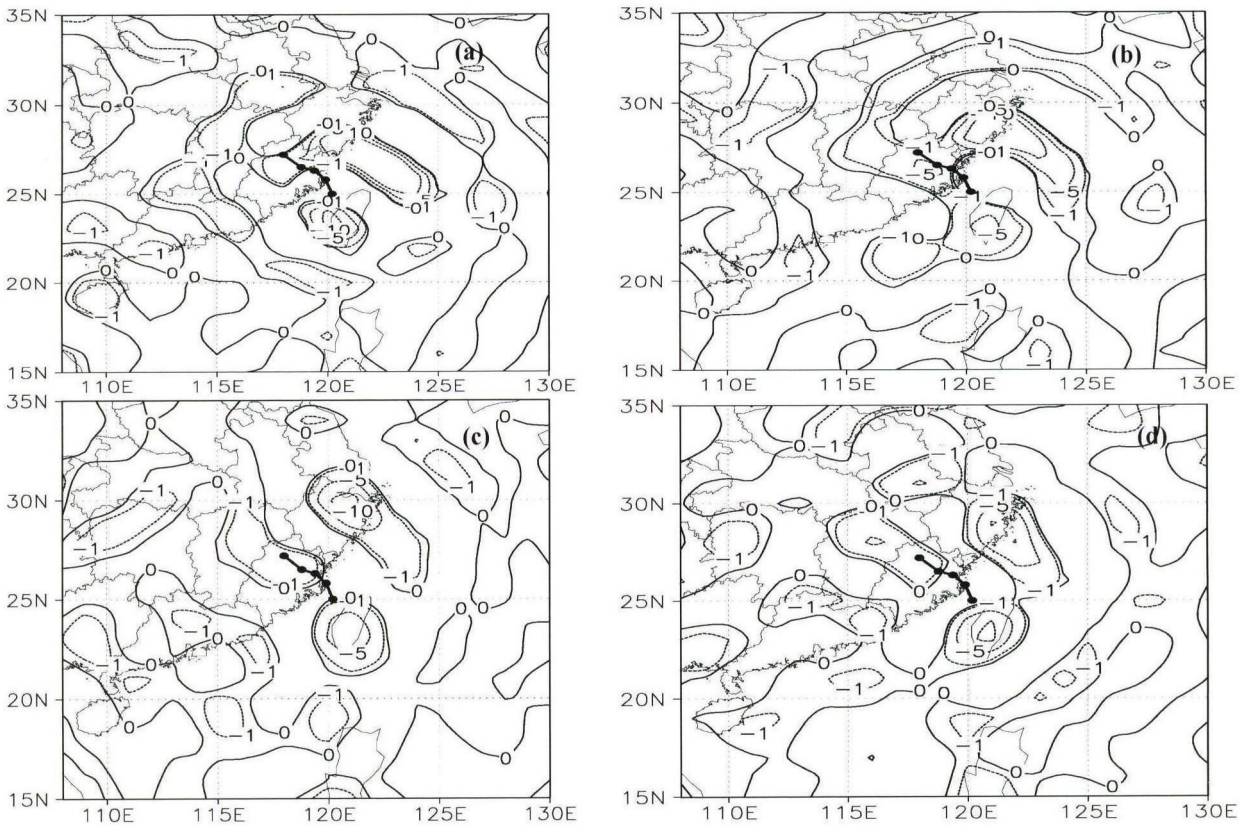

Figure 9. Same as Fig.3, except for convergence field of $\frac{R_d}{C_p \cdot p}\nabla^2(H)$ (unit: 10^{-15}hPa/s).

lower atmosphere on the right side of typhoon's track are much wider and stronger than counterparts on the left side, with obvious asymmetric distribution feature. The further analysis of Q vector partitioning shows that the forcing effect of mesoscale weather system in lower atmosphere is stronger than that of large-scale, which is more helpful to formation of the asymmetric distribution feature of precipitation in Fig.1b and Fig.2.

(3) There's diabatic heating effect in upper and lower atmosphere, and the range and intensity of diabatic heating effect present certain asymmetric distribution feature referring to typhoon path.

According to above, humidity condition in upper atmosphere, forcing effect of lower atmosphere on vertical ascending motion, especially the forcing effect of mesoscale weather system in lower atmosphere, and diabatic heating effect in upper and lower atmosphere, all present asymmetric distribution feature similar to counterparts of the precipitation from typhoon Haitang (2005), which shows the above factors are conducive to formation of asymmetric distribution feature of precipitation.

Furthermore, it also should be noted that the vertical advection term of Eq. (8) includes vertical motion with considering forcing effect of diabatic heating. Two aspects should be noted and considered as follows: (1) Laplace term of Eq.(8) reflects the relation between diabatic heating and vertical motion, i.e., the forcing effect of diabatic heating on vertical motion. However, the vertical motion is used for calculating adiabatic heating. Therefore, it is hard to distinguish the causality between them. (2) As vertical motion cannot be obtained from observation directly, the vertical motion will be different based on different diagnostic methods, thus, influencing the calculating result of vertical advection term in Eq. (8), and further influencing the quantitative description of diabatic heating forcing effect, that is to say, the different origin of vertical motion in Eq.(8) may result in difference of diabatic heating forcing effect. Therefore, while calculating Eq. (8), the calculating method or its origin of vertical motion should be specified clearly.

It needs to be pointed out that 700 hPa is the link for middle and low atmosphere, whose meteorological condition is closely related to the occurrence and development of weather system. The study of Yue is based on 700 hPa, and suggests that water vapor condition may not be the main factor for asymmetric distribution feature of precipitation from typhoon Haitang (2005)[24]. However, this paper is based on the average factor in upper and lower atmosphere, and 700 hPa is covered in lower atmosphere (1 000−600 hPa), meanwhile, the diagnostic result of lower atmosphere in section 3 is consistent with Yue[24]. Furthermore, this

paper further perfects the job of Yue [24] by careful and complete consideration of upper and lower atmosphere.

Finally, the formation reason of precipitation from landed typhoon is complicated, involving typhoon circulation structure, strength, track, moving speed, environment field and underlaying surface, each of the factors above is very important. This paper focuses on the effect of atmosphere factor, which does not mean that the effects of other factors are not important. In fact, the effect of each factor can not be neglected, especially topography effect. Atmosphere factor is just one of the many influencing factors, but not all.

REFERENCES:

[1] CHEN Lian-shou, XU Xiang-de, LUO Zhe-xian, et al. Introduction to Tropical Cyclone Dynamics [M]. Beijing: China Meteorological Press, 2002, 303-304 (in Chinese).

[2] CHEN Lian-shou, LUO Zhe-xian, LI Ying. Research advances on tropical cyclone landfall process [J]. Acta Meteorol Sinica, 2004, 62(5): 541-549 (in Chinese).

[3] CHENG Zheng-quan, CHEN Lian-shou, XU Xiang-de, et al. Research progress on typhoon heavy rainfall in China for last ten years [J]. Meteorol Mon, 2005, 31(12): 3-9 (in Chinese).

[4] CLINE I M. Tropical Cyclones [M]. Macmillan Co., 1926, 301pp.

[5] KOTESWARAM P, GASPAR S. The surface structure of tropical cyclones in the Indian area [J]. Ind J Meteorol Geophys, 1956, 7: 339-352.

[6] MILLER B I. Rainfall rates in Florida hurricanes [J]. Mon Wea Rev, 1958, 86(7): 258-264.

[7] FRANK W M. The structure and energetics of the tropical cyclone. Part I: Storm structure [J]. Mon Wea Rev, 1977, 105(9): 1 119-1 135.

[8] PARRISH J R, BURPEE R W, MARKS F D. Rainfall patterns observed by digitized radar during the landfall of Hurricane Frederic (1979) [J]. Mon Wea Rev, 1982, 110 (12): 1 933-1 944.

[9] ELSBERRY R L. Predicting hurricane landfall precipitation: Optimistic and pessimistic views from the symposium on precipitation extremes [J]. Bull Amer Meteorol Soc, 2002, 83(9): 1 333-1 339.

[10] BURPEE R W, BLACK M L. Temporal and spatial variations of rainfall near the centers of two tropical cyclones [J]. Mon Wea Rev, 1989, 117(10): 2 204-2 218.

[11] TAO Zu-yu, TIAN Bai-ping, HUANG Wei. Asymmetry structure and torrential rain of landing typhoon 9216 [J]. J Trop Meteorol, 1994, 10(1): 69-77 (in Chinese).

[12] DING Jin-cai, YAO Zu-qing, TANG Xin-zhang. The analysis of the asymmetric structure of tropical cyclone Doug and its influence on precipitation [J]. Acta Meteorol Sinica, 1997, 55(3): 379-384 (in Chinese).

[13] ATALLAH E, BOSART L F, AIYYER A R. Precipitation distribution associated with landfalling tropical cyclones over the eastern United States [J]. Mon Wea Rev, 2007, 135(6): 2 185-2 206.

[14] TULEYA R E, KURIHARA Y. A numerical simulation of the landfall of tropical cyclones [J]. J Atmos Sci, 1981, 35(2): 242-257.

[15] BENDER M A, TULETA R E, KURIHARA Y. A numerical study of the effect of a mountain range on a landfalling tropical cyclone [J]. Mon Wea Rev, 1985, 113 (4): 567-582.

[16] WU C C, YEN T H, KUO Y H, et al. Rainfall simulation associated with typhoon Herb (1996) near Taiwan. Part I: The topographic effect [J]. Wea Forecasting, 2002, 17(5): 1 001-1 015.

[17] CHEN Y S, YAU M K. Asymmetric structures in a simulated landfalling hurricane [J]. J Atmos Sci, 2003, 60(18): 2 294-2 312.

[18] LV Mei, ZOU Li, YAO Ming-ming, et al. Analysis of asymmetrical structure of precipitation in typhoon Aere [J]. J Trop Meteorol, 2009, 25(1): 22-28 (in Chinese).

[19] YUAN Jin-nan, ZHOU Wen, HUANG Hui-jun. Observational analysis of asymmetric distribution of convection associated with tropical cyclone "Chanchu" and "Prapiroon" making landfall along the south China coast [J]. J Trop Meteorol, 2009, 25(4): 385-393 (in Chinese).

[20] DING Zhi-ying, WANG Yong, SHEN Xin-yong, et al. On the causes of rainband breaking and asymmetric precipitation in typhoon Haitang (2005) before and after its landfall [J]. J Trop Meteorol, 2009, 25 (5): 513-520 (in Chinese).

[21] WANG Yong, DING Zhi-ying, LI Xun, et al. Dynamic analysis of asymmetric spiral rain bands around the landing of typhoon Haitang (2005) [J]. J Trop Meteorol, 2010, 26(5): 544-554 (in Chinese).

[22] XU Xiang-chun, YU Yu-bin, WANG Shi-gong, et al. Analysis of causation of asymmetric precipitation associated with strong typhoon "Damrey" [J]. J Trop Meteor, 2012, 28(5): 687-697 (in Chinese).

[23] YUE Cai-jun, SHOU Shao-wen, ZENG Gang, et al. Preliminary study on asymmetric cause of formation of precipitation associated with typhoon Haitang [J]. Plateau Meteorol, 2008, 27(6): 1 334-1 342 (in Chinese).

[24] YUE Cai-jun. A quantitative study of asymmetric characteristic genesis of precipitation associated with typhoon Haitang [J]. Chin J Atmos Sci, 2009, 33 (1): 51-70 (in Chinese).

[25] ZHANG Xing-Wang. The expression of the modified Q vector and its application [J]. J Trop Meteorol, 1999, 15 (2): 162-167 (in Chinese).

[26] KEYSER D, REEDER M J, REED R J. A generalization of Petterssen's frontogenesis function and its relation to the forcing of vertical motion [J]. Mon Wea Rev, 1988, 116(3-4): 762-780.

[27] KEYSER D, STCHMIDT B D, DUFFY D G. Quasi-geostrophic vertical motions diagnosed from along- and cross-isentrope components of the Q vector [J]. Mon Wea Rev, 1992, 120(5): 731-741.

[28] KURZ M. Synoptic diagnosis of frontogenetic and cyclogenetic processes [J]. Meteorol Atmos Phys, 1992, 48(1): 77-91.

[29] KURZ M. The role of frontogenetic and frontolytic wind field effects during cyclonic development [J]. Meteorol Appl, 1997(4): 353-363.

[30] BARNES S L, COLMAN B R. Quasigeostrophic diagnosis of cyclogenesis associated with a cut off extratropical cyclone - The Christmas 1987 storm [J]. Mon Wea Rev, 1993, 121(6): 1 613-1 634.

[31] BARNES S L, COLMAN B R. Diagnosing an operational numerical model using Q-vector and potential vorticity concepts [J]. Wea Forecast, 1994, 9(1): 85-102.

[32] SCHAR C, WERNLI H. Structure and evolution of an isolated semi-geostrophic cyclone [J]. Quart J Roy Meteorol Soc, 1993, 119(509): 57-90.

[33] MARTIN J E. Quasi-geostrophic forcing of ascent in the occluded sector of cyclones and the trowel airstream [J]. Mon Wea Rev, 1999, 127(1): 70-88.

[34] MARTIN J E. Lower-tropospheric height tendencies associated with the shearwise and transverse components of quasigeostrophic vertical motion [J]. Mon Wea Rev, 2007, 135(7): 2 803-2 809.

[35] YUE C J, SHOU S W, LIN K P, et al. Diagnosis of the heavy rain near a Meiyu front using the wet Q vector partitioning method [J]. Adv Atmos Sci, 2003, 20(1): 37-44.

[36] YUE Cai-jun, DONG Mei-ying, SHOU Shao-wen, et al. Improved wet Q vector's analytical method and the mechanism of Meiyu front rainstorm genesis [J]. Plateau Meteorol, 2007, 26(1): 165-175 (in Chinese).

[37] YUE Cai-jun, LU Xiao-qin, Li Xiao-fan, et al. A study of partitioning Q vector on background conditions of a torrential rainfall over Shanghai, China on 25 August 2008 [J]. J Trop Meteorol, 2011, 17 (3): 231-247 (in Chinese).

[38] PYLE M E, KEYSER D, BOSART L F. A diagnostic study of jet streaks: Kinematic signatures and relationship to coherent tropopause disturbances [J]. Mon Wea Rev, 2004, 132(1): 297-319.

[39] POSSELT D J, MARTIN J E. The effect of latent heat release on the evolution of a warm occluded thermal structure [J]. Mon Wea Rev, 2004, 132(2): 578-599.

[40] WANG Chuan, DU Chuan-li, SHOU Shao-wen. Application of Q-vector theory to "02.6" heavy storm rain on the east side of Qinghai-Xizhang Plateau [J]. Plateau Meteorol, 2005, 24(2): 261-267 (in Chinese).

[41] YANG Xiao-xia, SHEN Tong-li, LIU Huan-zhu, et al. Application of the wet Q vector partitioning method to the diagnosis of the heavy rainstorm [J]. Plateau Meteorol, 2006, 25(3): 464-475 (in Chinese).

[42] THOMAS B C, MARTIN J E. A synoptic climatology and composite analysis of the Alberta Clipper [J]. Wea Forecasting, 2007, 22(2): 315-333.

[43] LIANG Lin-lin, SHOU Shao-wen, MIAO Chun-sheng. Diagnostic analysis of a Meiyu front heavy rain process in July 2005 using wet Q vector partitioning theory [J]. J Nanjing Inst Meteorol, 2008, 31 (2): 167-175 (in Chinese).

[44] YUE Cai-jun. Quantitative analysis of torrential rainfall associated with typhoon landfall: A case study of typhoon Haitang (2005) [J]. Progr Nat Sci, 2009, 19(1): 55-63 (in Chinese).

Citation: YUE Cai-jun, CAO Yu, GU Wen et al. Study on the genesis of asymmetrical distribution characteristics of precipitation associated with the typhoon Haitang (2005) from the view of atmospheric factor [J]. J Trop Meteorol, 2016, 22(3): 265-276.